

XMM-Newton CCF Release Note

XMM-CCF-REL-393

EPIC MOS CTI Update

M.J.S. Smith & M. Stuhlinger

July 13, 2023

1 CCF Components

Name of CCF	VALDATE	EVALDATE	Blocks Changed	XSCS Flag
EMOS1_CTL_0100.CCF	2018-10-30T06:00:00		CTI_EXTENDED	NO
EMOS2_CTL_0104.CCF	2018-10-30T06:00:00		CTI_EXTENDED	NO

2 Changes

The MOS energy scale correction is implemented in the calibration on an epochal basis, a new epoch being defined whenever the modelled time dependency no longer yields an adequate energy reconstruction for newly collected data. This release concerns a new epoch, modelling the long-term charge transfer inefficiency (LTCTI) trend starting from revolution 3460 (2018-10-30T06:00:00), and based on data accumulated up to revolution 4138 (July 2022).

The correction for the time-evolution of the MOS energy scale, mainly due to degradation of the charge transfer efficiency, is based on analysis of CalClosed exposures in which the detector is illuminated by the on-board radioactive Fe-55 source, producing emission lines at the Al K α (1486.57 eV, Suresh 2000), Mn K α and Mn K β (5895.75 eV and 6489.97 eV, respectively, Holzer 1997) energies.

Up to recently, the epoch-dependent parameters which describe the energy scale (gain offset, gain slope, serial and parallel LTCTI) were derived through a simultaneous solution, where the respective CTI values were determined through a sufficiently fine spatial analysis of the measured line energies across the detector (see Stuhlinger 2019a and 2019b for the most recent previous updates). However, owing to the natural decay of the radioactive calibration source, it has in recent times become ever harder to obtain sufficient data to allow such direct measurements of the CTI, and determine sufficiently constrained values for both CTI and gain components simultaneously.

This is especially problematic for MOS1, where the calibration source illumination is substantially weaker than in MOS2.

Therefore a new scheme to derive the energy scale correction has been put in place, the so-called “*empirical LTCTI correction*”. In this method, for the new epoch the parallel LTCTI parameters are derived which yield the best *CCD-averaged* reconstruction of the energy scale, while the respective gain offset, gain slope and serial LTCTI descriptions are assumed to be unchanged with respect to the values derived for the most recent epoch. The justification of this choice is that of the two CTI effects, the parallel is the larger (by a factor of approximately 3), with historically a greater dependence on time. The serial CTI describes charge shifts in the shielded frame store area and its temporal evolution is shown to be more stable across epochs.

As of SAS 7.0, the MOS energy reconstruction is determined as per the following algorithm:

$$E' = E + RAWX * CTIX + RAWY * CTIY - OFFSET(RAWX, RAWY)$$

$$E'' = gain_0 + gain_1 * E'$$

with:

$$CTIX(E, t) = (A_0 + A_1 * t) * E^\alpha$$

$$CTIY(E, t) = (B_0 + B_1 * t) * E^\beta$$

and where:

E :	uncorrected PHA value
E' :	CTI corrected PHA value
E'' :	PI value
$RAWX, RAWY$:	event raw pixel coordinates
$OFFSET$:	specific column segment dependent offsets
$CTIX$:	serial CTI
$CTIY$:	parallel CTI
t :	time
A_0, A_1, α :	parameters which describe time and energy dependent serial CTI
B_0, B_1, β :	parameters which describe time and energy dependent parallel CTI
$gain_0, gain_1$:	gain offset and slope

In the empirical LTCTI correction scheme, the parameters $A_0, A_1, \alpha, gain_0, gain_1$ and $OFFSET$ are fixed to their respective values as derived for the most recent epoch, and are thus assumed to be valid for the new epoch. The parameters B_0, B_1 and β are then left as free parameters in a fit of the above functions to minimise the differences between the resulting CCD-averaged E'' and the expected E_{lab} values.

These parameters have been derived for recent data up to revolution 4138 (see Table 1) and included in a new set of EMOS CTI CCFs which, in conjunction with the existing EMOS ADU CONV

		B_0	B_1 (s^{-1})	β
MOS1	CCD1	-5.176e-05	1.755e-12	0.5541
	CCD2	-9.647e-04	2.788e-12	0.5661
	CCD4	1.664e-05	8.934e-13	0.6137
	CCD5	-9.018e-04	2.493e-12	0.6140
	CCD7	1.402e-04	1.126e-12	0.5496
MOS2	CCD1	-2.736e-04	1.353e-12	0.6011
	CCD2	-3.344e-05	7.230e-13	0.6619
	CCD3	-1.217e-04	2.394e-12	0.4945
	CCD4	-3.112e-04	1.248e-12	0.6222
	CCD5	-5.919e-04	1.912e-12	0.5986
	CCD6	-3.019e-04	1.777e-12	0.5669
	CCD7	-4.486e-04	2.547e-12	0.5093

Table 1: The best fit parameters which describe the time and energy dependent parallel CTI for the epoch covered by this CCF release.

CCFs, describe the energy scale correction for the epoch mentioned previously. For wider context, Figs. 5 and 6 in Appendix A show the evolution of the parameterised CTI over the full set of epochs covering the mission.

3 Scientific Impact and Estimated Quality

Compared with the previous calibration, the new CCFs yield a significant improvement of the MOS energy scale reconstruction at Al $K\alpha$ and Mn $K\alpha$ for the most recent epoch. A comparison of results obtained with old and new calibration in the latest epoch is shown in Figs 1 to 4. The general trend in ever greater energy under-correction (by up to $\sim 15 - 20$ eV at Al $K\alpha$ and $\sim 20 - 30$ eV at Mn $K\alpha$), seen in the old calibration, has now been very much reduced or removed. For all but the most recent data, up to \sim revolution 4145, and for most CCDs, the new CCFs yield an accuracy of the energy reconstruction to within ± 5 eV at Al $K\alpha$ and ± 10 eV at Mn $K\alpha$.

However, for the more recent data, which were not used in the derivation of the LTCTI parameters, increasing deviations are seen. Depending on CCD, these are characterised by a trend to increased energy under-correction. An exception is MOS2 CCD4, which shows an apparent step in the gain after the July 2022 eclipse season, leading to a systematic overcorrection by ~ 20 eV. These inaccuracies will need to be corrected in a future calibration update for a new epoch.

A main concern is that the empirical LTCTI correction method, being derived and validated against data averaged across the full CCD, while yielding a correct CCD averaged energy scale, may not sufficiently remove spatial dependencies. To this end, the spatial accuracy of the energy scale was investigated, by examining reconstructed energies averaged over a 3×3 grid of $\sim 200 \times 200$ pixels each, per CCD. Owing to insufficient data and resulting large uncertainties in the most recent epochs, as a test, the empirical LTCTI correction was applied to *all* previous epochs (post cooling) to compare the accuracy that could be obtained with the new versus the old method. Results show that the spatial dependency is similar within errors and that the empirical method does not

introduce unwanted spatial artefacts, at least on the, albeit rough, spatial scale investigated.

An additional concern is the validity of the assumed gain parameters for the new epoch. At energies below the Al $K\alpha$ calibration line, this was tested on the routine calibration target 1E 0102.2-7219, a compact SNR with prominent emission features, which was observed in the new epoch. Using an IACHEC defined model (Plucinsky et al. 2017), a comparison was made of the quality of fit at the O VII, O VIII, Ne IX and Ne X emission lines against data processed with old and new EMOS CTI CCFs. For the new epoch, the empirical LTCTI correction yielded similar results for MOS1 and marginally improved fits for MOS2. However, it is noted that, as this target is observed at or close to the nominal aim point, this test is only useful as validation of the accuracy of the CCD1 energy scale.

4 Expected Updates

Owing to the continuous evolution of the MOS LTCTI and gain, periodic updates of the energy scale correction based on newly accumulated data will be necessary.

In addition, investigations are underway into whether there is sufficient data to allow an extension of the empirical correction to include serial LTCTI and / or gain components.

5 Test Procedures and Results

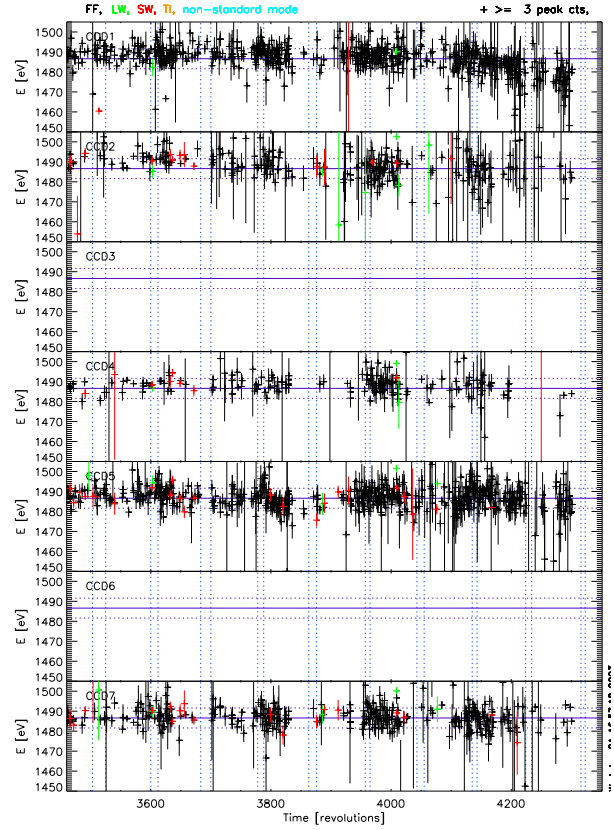
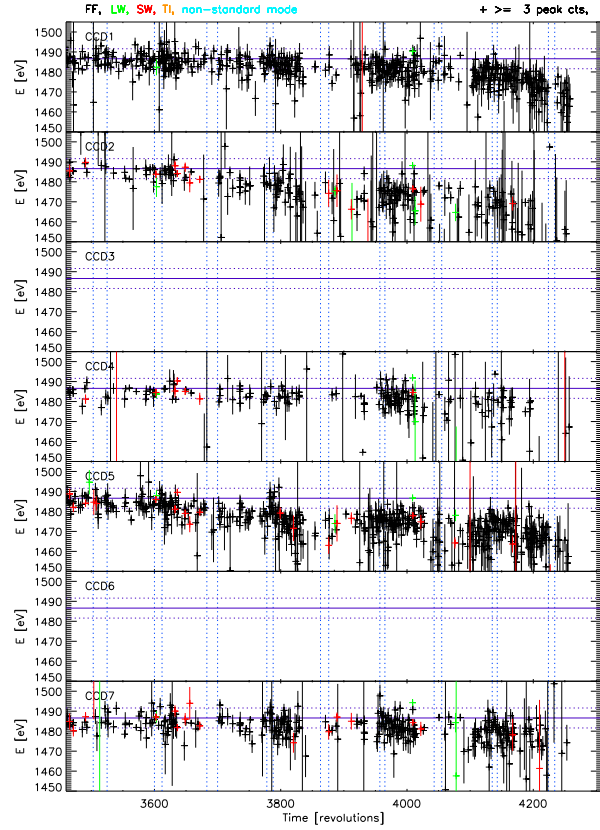
Correct functionality tested with `cifbuild` and `emproc` (SAS version 20.0.0).

6 References

- Holzer et al. 1997, Phys. Rev. A, 56, 6
Plucinsky, P. et al. 2017, A&A 597, A35
Stuhlinger, M. 2019a, Update of EPIC MOS CTI, Tech. Rep. XMM-CCF-REL-363, XMM SOC
<https://xmmweb.esac.esa.int/docs/documents/CAL-SRN-0363-1-1.pdf>
Stuhlinger, M. 2019b, Update of EPIC MOS gain, Tech. Rep. XMM-CCF-REL-364, XMM SOC
<https://xmmweb.esac.esa.int/docs/documents/CAL-SRN-0364-1-0.pdf>
Suresh et al. 2000, J. Phys. B. At. Mol. Opt. Phys. 33

MOS1 AI-K PATTERN==0

MOS1 AI-K PATTERN==0



MOS1 AI-K PATTERN in [0:12]

MOS1 AI-K PATTERN in [0:12]

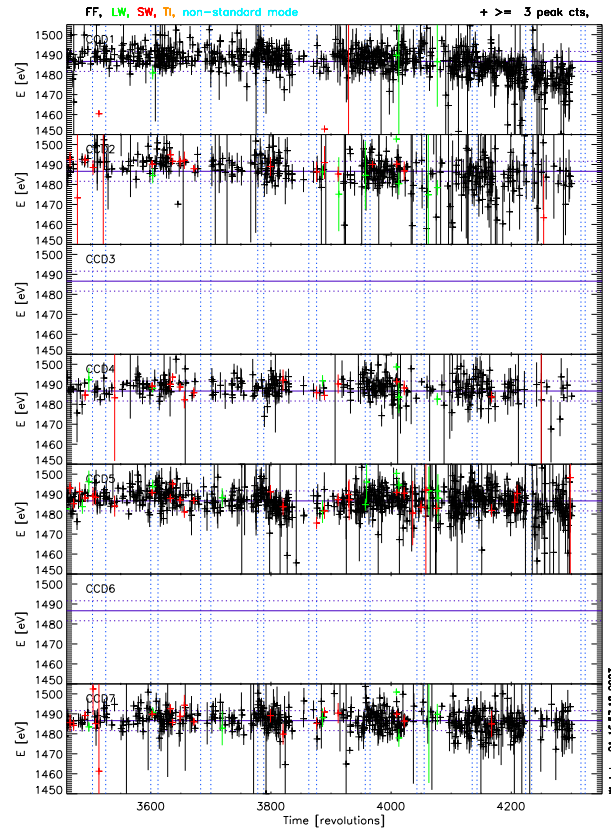
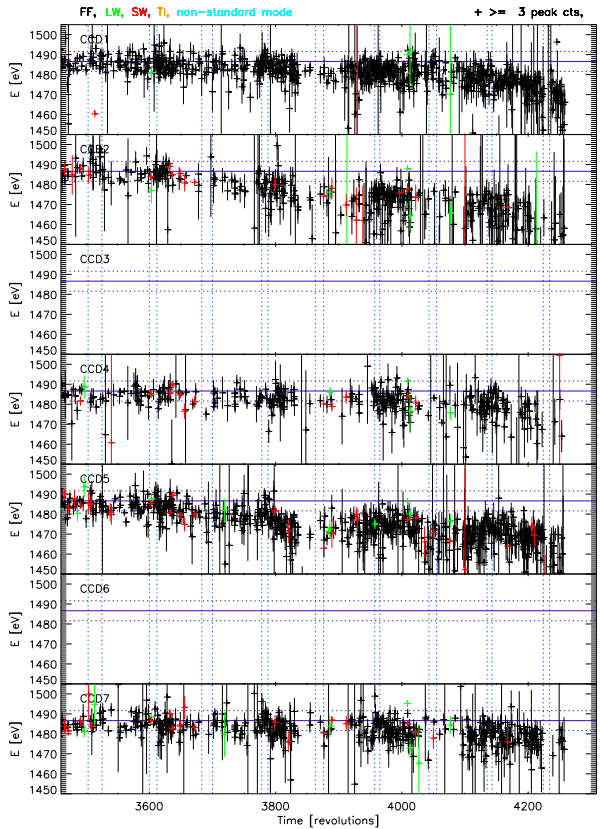


Figure 1: MOS1 AI $K\alpha$ line energy scale comparing old and new CCFs in left and right column respectively. Top row is for singles, bottom row for patterns 0-12. Eclipse seasons are indicated by vertical blue lines, CCF epochs by red lines. The horizontal solid line represents the laboratory line energy, the dotted lines the ± 5 eV range.

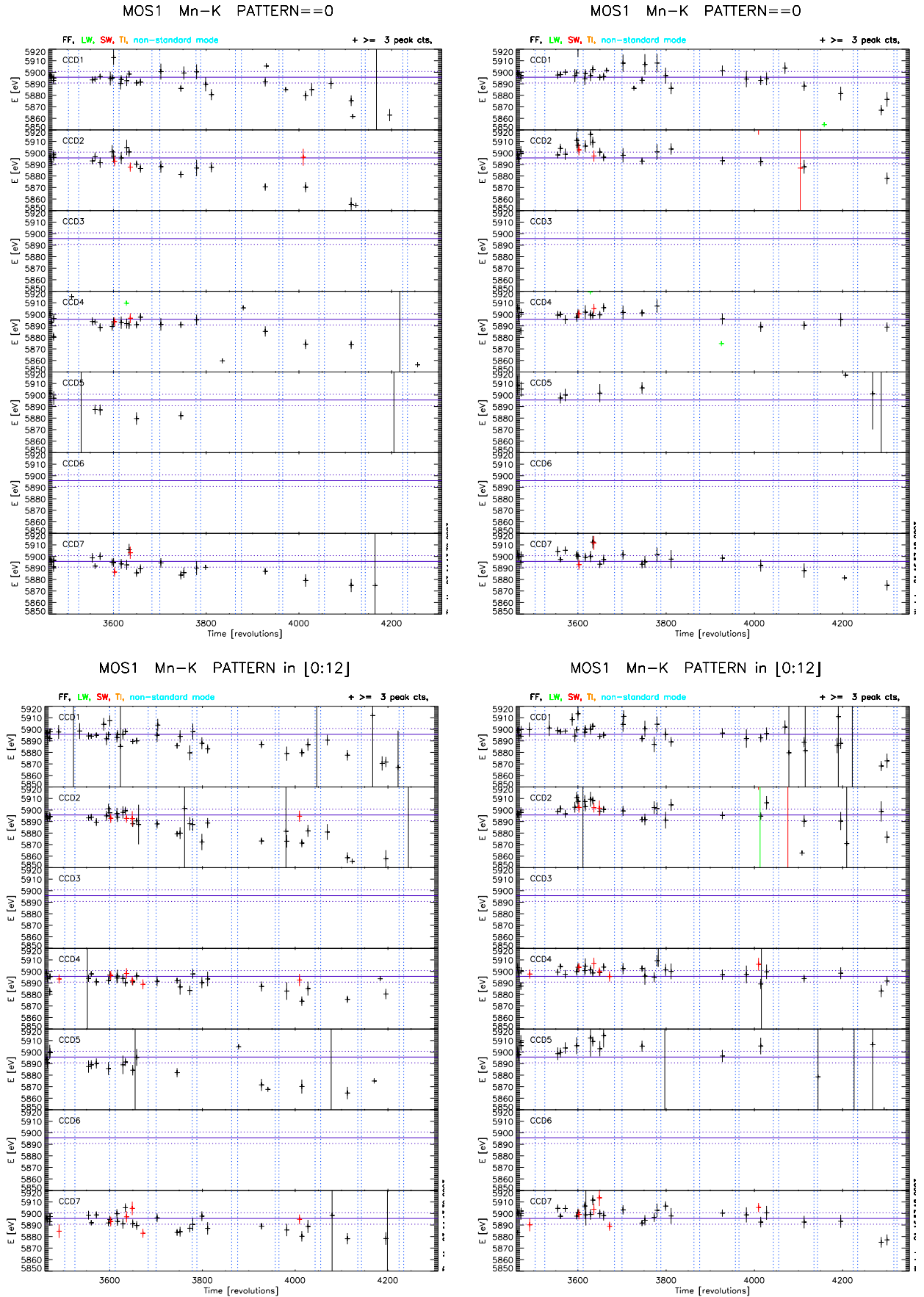


Figure 2: As Fig. 1, but for MOS1 at Mn K α .

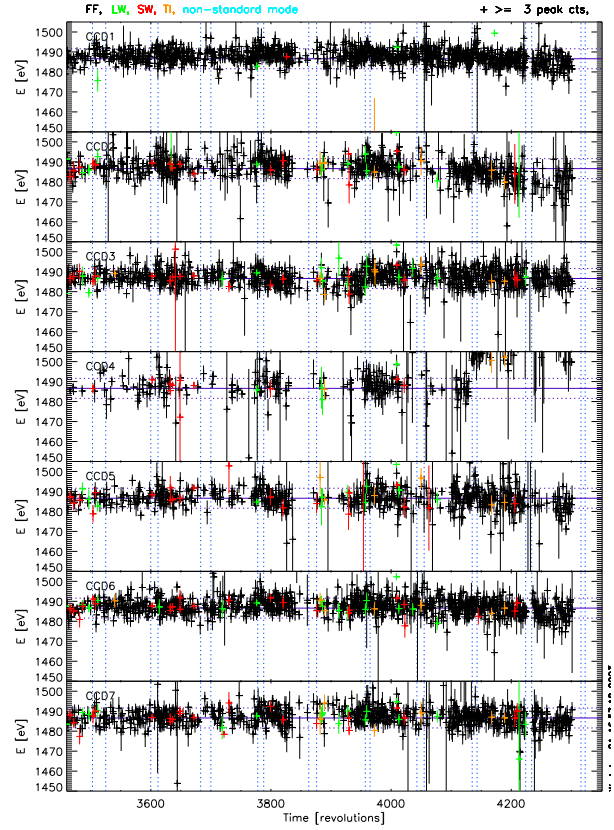
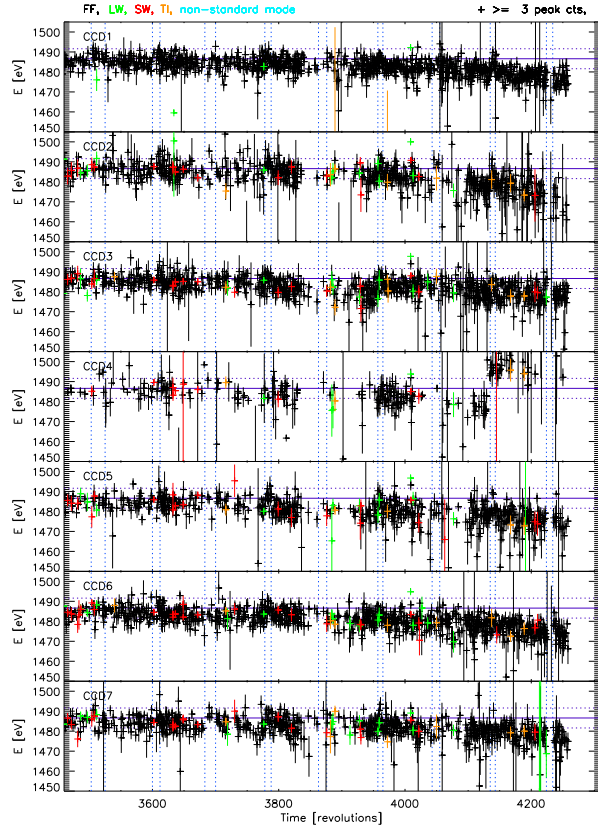
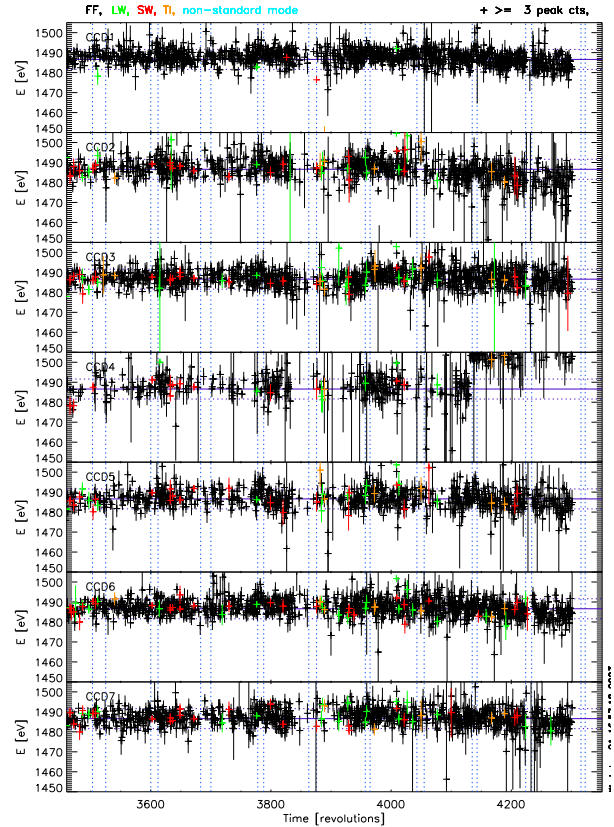
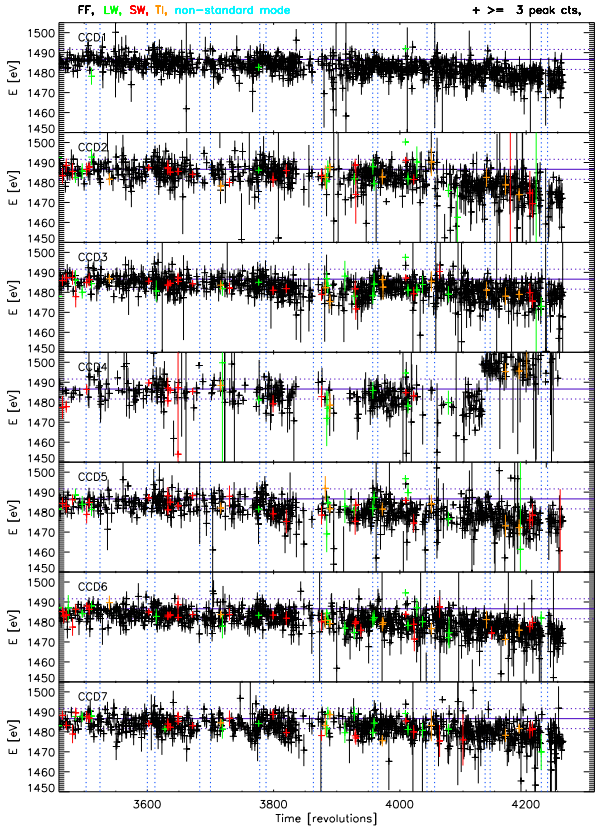
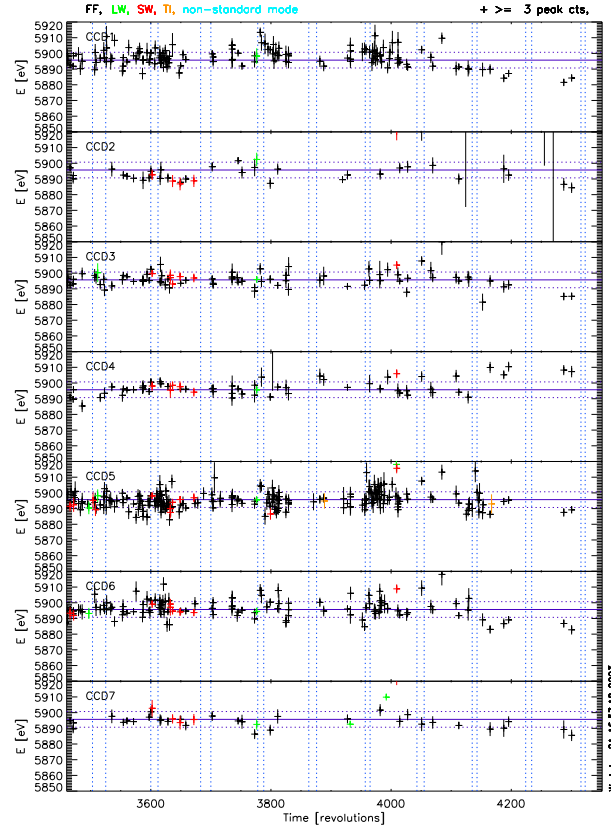
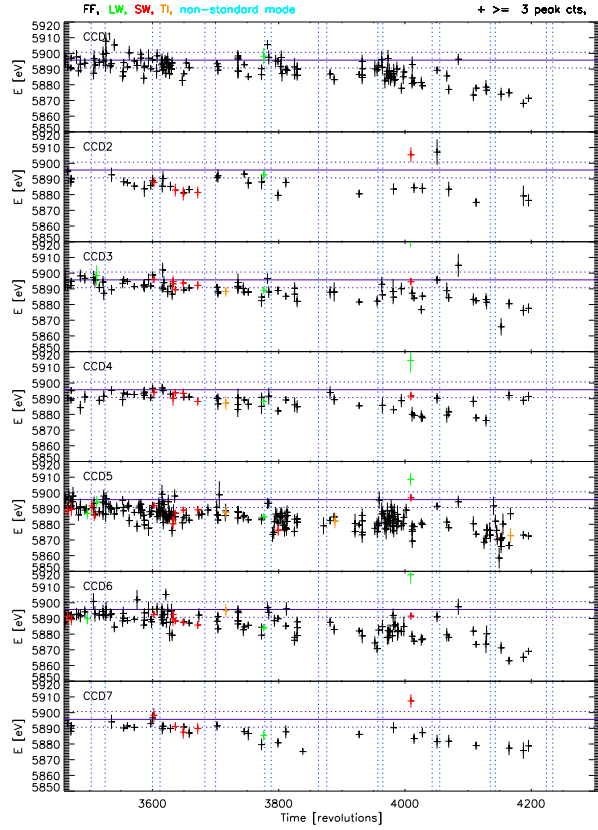
MOS2 AI-K PATTERN==0
MOS2 AI-K PATTERN==0

MOS2 AI-K PATTERN in [0:12]
MOS2 AI-K PATTERN in [0:12]


Figure 3: As Fig. 2, but for MOS2 at Al K α .

MOS2 Mn-K PATTERN==0

MOS2 Mn-K PATTERN==0



MOS2 Mn-K PATTERN in [0:12]

MOS2 Mn-K PATTERN in [0:12]

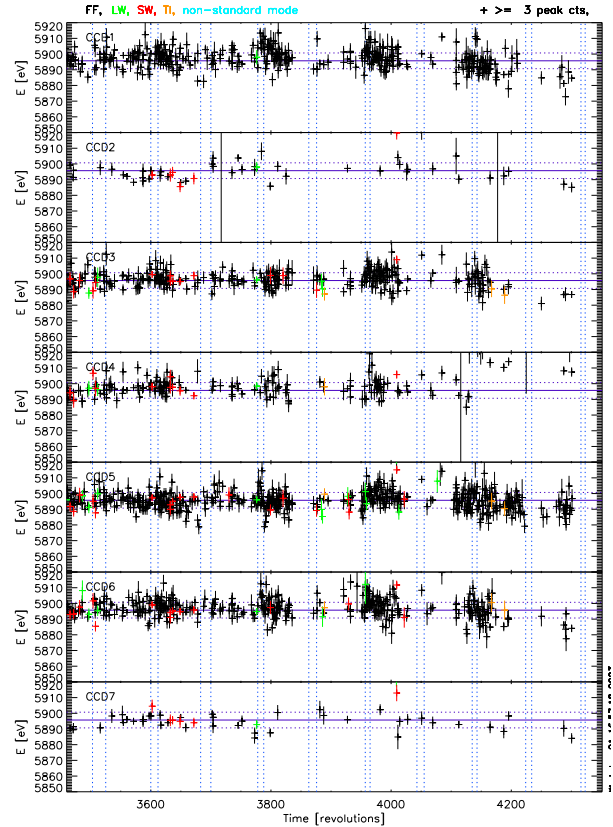
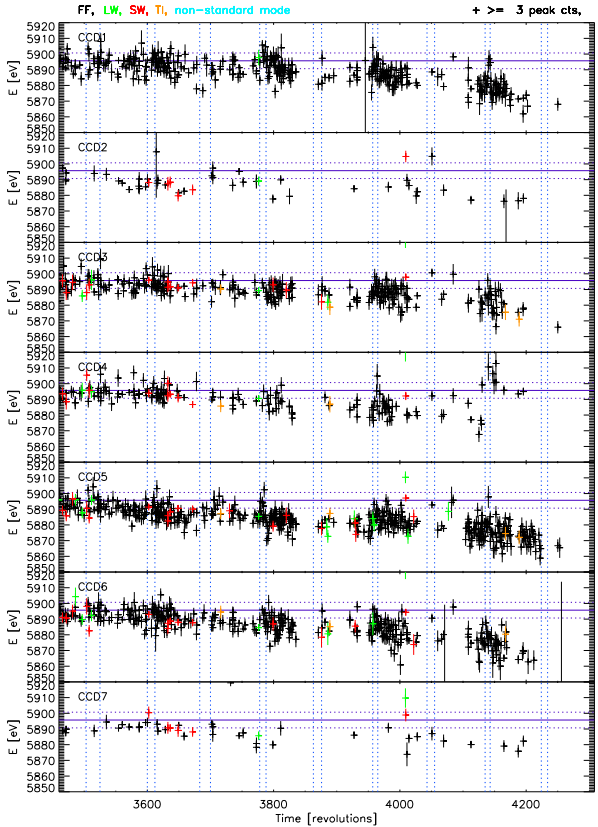


Figure 4: As Fig. 1, but for MOS2 at Mn $K\alpha$.

A Evolution of the parameterised CTI

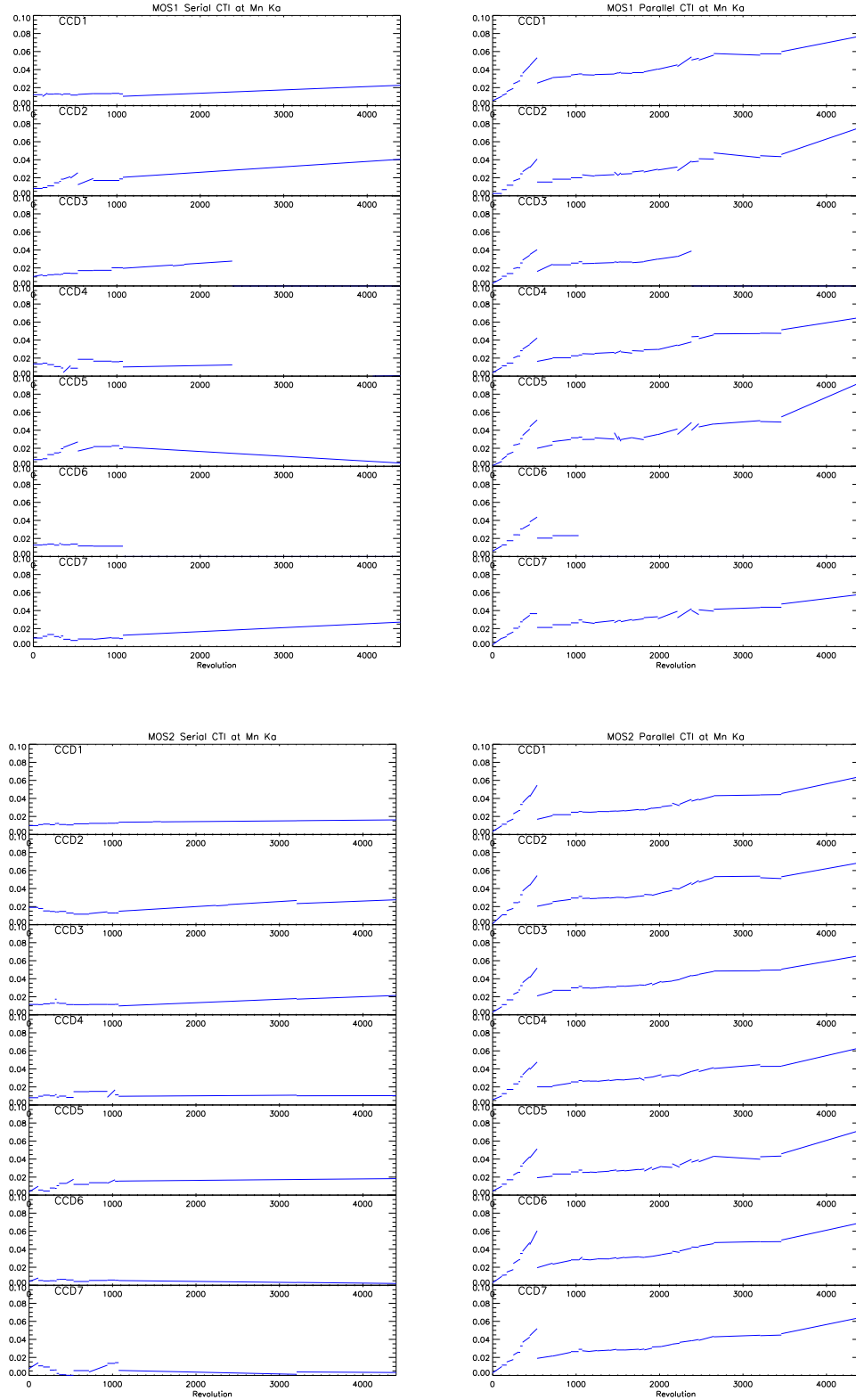


Figure 5: Evolution of the parameterised serial (left) and parallel (right) CTI, per CCD (top to bottom) at Mn $K\alpha$. Top row: MOS1, bottom row: MOS2.

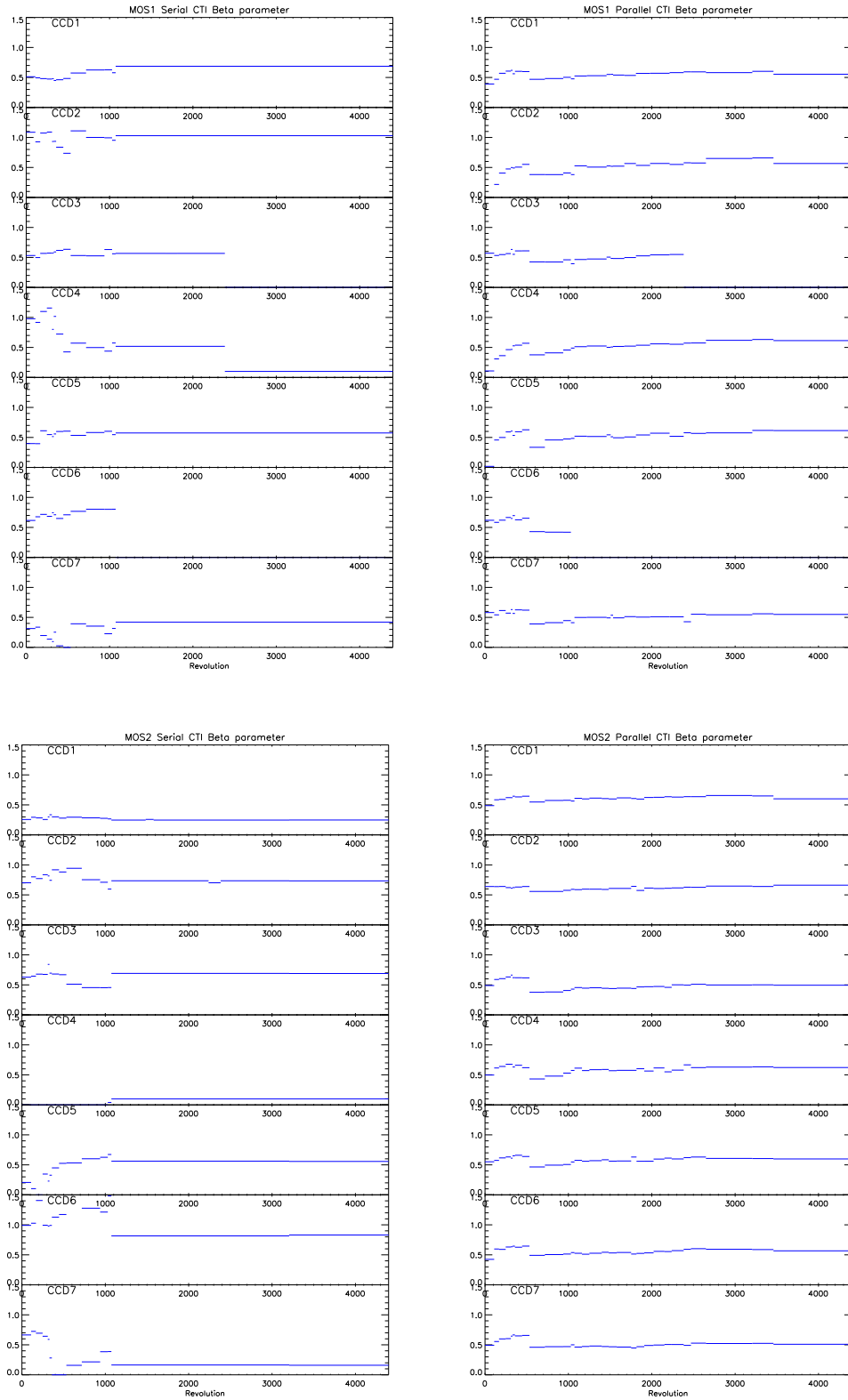


Figure 6: Evolution of the β parameter for the serial (left) and parallel (right) CTI, per CCD (top to bottom). Top row: MOS1, bottom row: MOS2.